arXiv:1607.07543v1 [cs.SY] 26 Jul 2016

Task-space coordinated tracking of multiple heterogeneous manipulators via controller-estimator approaches

Ming-Feng Ge[a], Zhi-Hong Guan[a], Chao Yang[a], Chao-Yang Chen[b], Ding-Fu Zheng[a], Ming Chi[a]

[a] *College of Automation, Huazhong University of Science and Technology, Wuhan, 430074, China*

[b] *School of Information and Electrical Engineering, Hunan University of Sience and Technology Xiangtan, Hunan, 411201, China*

Abstract

This paper studies the task-space coordinated tracking of a time-varying leader for multiple heterogeneous manipulators (MHMs), containing redundant manipulators and nonredundant ones. Different from the traditional coordinated control, distributed controller-estimator algorithms (DCEA), which consist of local algorithms and networked algorithms, are developed for MHMs with parametric uncertainties and input disturbances. By invoking differential inclusions, nonsmooth analysis, and input-to-state stability, some conditions (including sufficient conditions, necessary and sufficient conditions) on the asymptotic stability of the task-space tracking errors and the subtask errors are developed. Simulation results are given to show the effectiveness of the presented DCEA.

Keywords: task-space coordinated tracking, multiple heterogeneous manipulators (MHMs), redundant manipulator, distributed controller-estimator algorithm (DCEA).

Email addresses: fmgabc@163.com (Ming-Feng Ge[a]), zhguan@mail.hust.edu.cn (Zhi-Hong Guan[a])

Citation: Journal of The Franklin Institute, 2016, DOI: 10.1016/j.jfranklin.2016.06.025

1. Introduction

Coordinated control has been diffusely invoked in many practical applications of multiple manipulators, including coordination of bilateral human-swarm systems [1], single-master-multiple-slaves teleoperation [2], dual-user shared teleoperation [3]-[6], multi-robot teleoperation [7]-[10], multi-fingered grasping and manipulation [11, 12], due to their prominent superiority comparing with traditional centralized control, such as stronger stability, less energy consumption, greater operational efficiency [13]-[24].

Existing works focused on joint-space synchronization of two manipulators, namely, master-slave bilateral teleoperators, using various control technologies, such as adaptive control, passivity-based control, proportional-derivative control [25]-[28]. However, the single-master-single-slave framework containing two manipulators is already too simple for some complicated practical tasks. By invoking cooperative concurrent control, synchronization of interconnected Lagrangian systems had been investigated [29]. Distributed containment control had been developed for nonlinear multi-agent systems in the presence of dynamical uncertainties and external disturbances and applied to Lagrangian networks [30]. However, the kinematics of robotic manipulators had not been taken into consideration in the above literatures. In reality, task-space algorithms considering kinematics of manipulators are more practical and applicative comparing with joint-space algorithms. It thus motivates a group of researches on task-space algorithms. In presence of kinematic and dynamic uncertainties, task-space synchronization had been addressed for multiple manipulators under strong connected graphs by invoking passivity control [31] and adaptive control [32]. Note that the above literatures mainly focuses on motion control of kinematically identical and nonredundant robotic manipulators with parametric uncertainties.

Redundant manipulators can achieve more performance benefits in contrast to nonredundant ones [33, 34]. On the other hand, multiple manipulators containing both redundant and nonredundant individuals, namely, multiple heterogeneous manipulators (MHMs), are necessary and inevitable in some natural and man-made systems, *e.g.*, human hands and multi-fingered hands [11, 12]. Inspired by conceivable performance benefits of MHMs, task-space synchronization of MHMs under balanced connected topologies had been achieved via the passivity control technology in [35], which can synchronize the combination signals of task-space position/velocity tracking errors to zero.

In this paper, we present some novel DCEA to achieve the task-space coordinated tracking of a time-varying leader for MHMs with parametric uncertainties and input disturbances, and the interaction topology of the MHMs are assumed to contain a spanning tree. The main contributions are summarised as follows. 1) Different from the coordination algorithms considering dynamics of Euler-Lagrange systems [29, 30], both the dynamics and kinematics are considered, which is more practical and challenging. 2) Different from the coordination algorithms for identical manipulators with a constant agreement value [31, 32], the tracking of a time-varying leader for MHMs is studied. 3) Different from balanced interaction topologies studied in [35], digraphs containing a spanning tree are invoked to describe the interaction topology. 4) The novel controller-estimator structure provides a theoretical guidance for coordinated control of various networked multi-agent systems, whose dynamics are complex and strong nonlinear.

The rest of the paper is structured as follows. In Section 2, the preliminaries are presented. In Section 3, the main results are presented. In Section 4, the simulations are given. In Section 5, the conclusion is proposed.

Notation: $\mathbb{R}^n$ represents the n-dimensional Euclidean space, I_n denotes the $n \times n$ identity matrix, $1_n = [1, \cdots, 1]^T$ represents the n-dimensional column vector, $\|\cdot\|$ represents the Euclidean norm, $\lambda_{\min}(\cdot)$ denotes the minimum eigenvalue of the corresponding matrix.

2. Preliminaries

2.1. Dynamics and Kinematics

The dynamics and kinematics of the ith individual in the MHMs with input disturbances are given as follows [33]:

$$\begin{cases} H_i(q_i)\ddot{q}_i + C_i(q_i, \dot{q}_i)\dot{q}_i + g_i(q_i) + d_i(t) = u_i, \\ \\ x_i = \psi_i(q_i),\ \dot{x}_i = J_i(q_i)\dot{q}_i, \end{cases} \tag{1}$$

where $i \in \mathcal{V} = \{1, \ldots, n\}$, $t \in \mathcal{Q} = [t_0, \infty)$, $t_0 \geq 0$ is the initial time, $q_i \in \mathbb{R}^{p_i}$ denotes the position in the joint space, $p_i \geq 2$ represents the degrees-of-freedom (DOF) of the ith manipulator, $H_i(q_i) \in \mathbb{R}^{p_i \times p_i}$ is the inertia matrix, $C_i(q_i, \dot{q}_i) \in \mathbb{R}^{p_i \times p_i}$ represents the centripetal-Coriolis matrix, $g_i(q_i) \in \mathbb{R}^{p_i}$ denotes the gravity vector, $d_i(t) \in \mathbb{R}^{p_i}$ represents the input disturbance, $u_i \in \mathbb{R}^{p_i}$ stands for the torque input, $x_i \in \Omega_x^i \subseteq \mathbb{R}^m$ denotes the

task-space position, Ω_x^i represents the work space, $\psi_i(q_i) \in \mathbb{R}^m$ denotes the forward kinematics, $m \geq 2$ denotes the task-space dimension and is thus the minimum number of DOF required to perform a given end-effector task, $J_i(q_i) = \partial\psi_i(q_i)/\partial q_i \in \mathbb{R}^{m\times p_i}$ stands for the Jacobian matrix.

The MHMs contain redundant manipulators and nonredundant ones, which means $\mathcal{V}$ consists of two subsets $\mathcal{E} = \{i \in \mathcal{V} \mid p_i = m\}$ and $\mathcal{F} = \{i \in \mathcal{V} \mid p_i > m\}$, *i.e.*, the manipulators in $\mathcal{E}$ are nonredundant and the ones in $\mathcal{F}$ are redundant. It is worthy to point out that a nonredundant manipulator has just a necessary number of DOF to perform a given end-effector task (*i.e.*, maintask) and a redundant manipulator has more DOF than the necessary number, which results in an infinite number of joint configurations to the inverse-kinematics problem. The redundancy can improve the functionality and flexibility of robotic manipulators and many subtasks (including manipulability enhancement, mechanical limit avoidance, and obstacle avoidance) can be obtained by choosing appropriate joint configurations. Then the following algebraic operation, that will be invoked hereinafter, is given by

$$J_i^\sharp = \begin{cases} J_i^{-1}, & i \in \mathcal{E}, \\ \\ J_i^\dagger, & i \in \mathcal{F}, \end{cases}$$

where for $i \in \mathcal{E}$, $J_i^\sharp = J_i^{-1} \in \mathbb{R}^{m\times m}$ denotes the normal inverse of $J_i(q_i)$; for $i \in \mathcal{F}$, $J_i^\sharp = J_i^\dagger = J_i^T(J_iJ_i^T)^{-1} \in \mathbb{R}^{p_i\times m}$ represents the pseudoinverse of $J_i(q_i)$ and satisfies the well-known Moore-Penrose conditions [36]. The following lemma that will be used hereinafter is given.

Lemma 1. *For $i \in \mathcal{F}$, the algebraic operation $J_i^\sharp$ satisfies*

$$J_i(I_{p_i} - J_i^\sharp J_i) = 0,\ (I_{p_i} - J_i^\sharp J_i)J_i^\sharp = 0,$$

$$(I_{p_i} - J_i^\sharp J_i)(I_{p_i} - J_i^\sharp J_i) = I_{p_i} - J_i^\sharp J_i.$$

For any $i \in \mathcal{V}$, the properties of system (1) are given as follows [35, 37].
(P1) $H_i(q_i)$ is positive definite. $\dot{H}_i(q_i) - 2C_i(q_i, \dot{q}_i)$ is skew symmetric;
(P2) The dynamic terms $H_i(q_i)$, $g_i(q_i)$, $d_i(t)$ are bounded for all possible q_i, and $\|C_i(q_i, \dot{q}_i)\| \leq \bar{c}_i\|\dot{q}_i\|$, where $\bar{c}_i > 0$ is a positive constant;
(P3) The dynamic terms can be parameterized, *i.e.*, $H_i(q_i)x + C_i(q_i, \dot{q}_i)y + g_i(q_i) = Y_i(q_i, \dot{q}_i, y, x)\vartheta_i$, where x, y are any proper vectors, $Y_i(q_i, \dot{q}_i, y, x)$ is the regressor and ϑ_i is a set of constant dynamic parameters.

Remark 1. *By the actual characteristics of MHMs, we assume that the kinematic terms $J_i(q_i)$ and $J_i^\sharp(q_i)$ are bounded; the kinematic singularities are avoided, i.e.,* $\mathrm{rank}(J_i^\sharp(q_i)) = m$*, for $i \in \mathcal{V}$. The above assumptions are the general properties of multiple manipulators, see [33, 37] for details.*

2.2. Graph Theory

The interaction of the MHMs is denoted by a digraph $\mathcal{G} = \{\mathcal{V}, \xi, \mathcal{A}\}$, where $\mathcal{V}$ is the node set, $\xi \subseteq \mathcal{V} \times \mathcal{V}$ is the edge set, $\mathcal{A} = [\varepsilon_{ij}]_{n\times n}$ is the weighted adjacency matrix with nonnegative adjacency elements. An edge in $\mathcal{G}$ is denoted by an ordered pair (v_i, v_j). $(v_i, v_j) \in \xi$ if and only if node j (*i.e.*, the jth manipulator) can directly access the information of node i. $\mathcal{N}_j = \{i \in \mathcal{V} \mid (v_i, v_j) \in \xi\}$ denotes the neighbor set of node j. $\mathcal{A}$ is defined as $i \in \mathcal{N}_j \Leftrightarrow \varepsilon_{ji} > 0$, otherwise $\varepsilon_{ji} = 0$, and $\varepsilon_{ii} = 0$, $\forall i, j \in \mathcal{V}$. $\mathcal{D} = diag\{d_1, \ldots, d_n\}$ is the degree matrix, where $d_i = \sum_{j\in\mathcal{N}_i} \varepsilon_{ij}$. The Laplacian matrix is defined as $\mathcal{L} = \mathcal{D} - \mathcal{A}$. A directed path is an ordered sequence $v_1, v_2, \cdots, v_\omega$ satisfying that any ordered pair of vertices appearing consecutively in the sequence is an edge of the digraph $\mathcal{G}$. A digraph contains a spanning tree if there exists a root node that has a directed path to all the other nodes. $\mathcal{B} = [b_1, \ldots, b_n]^T$ is the weight vector between the n nodes and the leader, where $b_i > 0$ if the states of the leader is available to node i, namely, node i is pinned; $b_i = 0$ otherwise. The states of the leader (node 0) x_0, v_0 and $a_0 \in \mathbb{R}^m$ satisfy $\dot{x}_0 = v_0$, $\dot{v}_0 = a_0$. The following assumptions that will be used hereinafter are given.

(A1) The leader has a directed path to all the nodes in $\mathcal{G}$ under $\mathcal{B}$;

(A2) $\|v_0\|_\infty < \beta_1$, $\|a_0\|_\infty < \beta_2$ and $\|\dot{a}_0\|_\infty < \beta_3$, where β_1, β_2 and β_3 are positive constants.

Remark 2. *By Assumption A2, the derivatives of the states of the leader x_0, v_0 and a_0 are bounded, which happens to be the actual characteristics of the trajectories that can be reachable by the real-world manipulators described by Euler-Lagrange equations [38].*

2.3. Problem Statement

The control tasks of this paper are presented in this section. It can be seen that for given $\dot{x}_i$, $\dot{x}_i = J_i(q_i)\dot{q}_i$ admits an infinite number of $\dot{q}_i$ when $i \in \mathcal{F}$ and only a single solution when $i \in \mathcal{E}$. Thus, to accomplish a given end-effector task, there exist only a single joint configuration for nonredundant manipulators and an infinite number of joint configurations for redundant

manipulators. Let the given end-effector task be called maintask and the tracking of a class of special joint configuration be called subtasks. Then the control tasks in this paper can be divided into the maintask and the subtask. Moreover, note that the nonredundant manipulators which have only one joint configuration for a given end-effector task (*i.e.*, maintask) cannot accomplish the subtasks.

Maintask: The maintask is to design distributed input u_i with the states of node i (the ith manipulator) and its neighbour set such that the task-space coordinated tracking can be accomplished, *i.e.*, $x_i \to x_0$ and $\dot{x}_i \to v_0$ as $t \to \infty$, $\forall i \in \mathcal{V}$.

Subtask: The subtask, *e.g.*, manipulability enhancement, mechanical limit avoidance, and obstacle avoidance, can only be accomplished by redundant manipulators. For different subtasks with respect to different redundant manipulators, we can construct a corresponding auxiliary vector $\varphi_i(t)$ to denote the gradients of some performance indices with respect to the corresponding subtask. Then the subtask for the ith manipulator is said to be achieved if $e_{si} \to 0$ as $t \to \infty$, where $i \in \mathcal{F}$, $e_{si} = (I_{p_i} - J_i^\sharp J_i)(\dot{q}_i - \varphi_i)$ denotes the subtask tracking error [39].

Remark 3. *The subtasks give more functional constraints on joint configurations and thus cannot be accomplished by nonredundant manipulators because they have only one joint configuration for their inverse-kinematics. Redundant manipulators have an additional DOF to accomplish the subtasks, which gives higher robustness and wider operational space comparing with nonredundant ones. However, the control design for redundant manipulators is more complex and challenging. Human arms, elephant trunks, and snakes are some examples of this kind of redundant system. The redundant is applicable in many practical applications and tough challenging in theoretical analysis [11, 12, 31].*

3. Task-space Coordinated Tracking of Multiple Heterogeneous Manipulators

This section studies the task-space coordinated tracking for MHMs with a time-varying leader, in which the position vector of the leader in the generalized coordinate is assumed to be bounded up to its third derivative, which is also invoked in [38].

3.1. Distributed Controller-Estimator Algorithms

In this section, DCEA for task-space coordinated tracking of MHMs are developed. Let $\hat{x}_i$, $\hat{v}_i$ and $\hat{a}_i \in \mathbb{R}^m$ be, respectively, the estimated value of x_0, v_0 and a_0 for the ith manipulator. Considering the heterogeneity of the MHMs, a joint-space auxiliary velocity $\dot{\hat{q}}_{ri} \in \mathbb{R}^{p_i}$ is given by

$$\dot{\hat{q}}_{ri} = J_i^\sharp(\hat{v}_i - \alpha_i(x_i - \hat{x}_i)) + (I_{p_i} - J_i^\sharp J_i)\varphi_i, \tag{2}$$

where α_i is a positive constant, $\varphi_i \in \mathbb{R}^{p_i}$ is the gradients of some performance indices with respect to the redundant manipulators. Then the joint-space auxiliary acceleration $\ddot{\hat{q}}_{ri}$ is defined as

$$\ddot{\hat{q}}_{ri} = \dot{J}_i^\sharp(\hat{v}_i - \alpha_i(x_i - \hat{x}_i)) + J_i^\sharp(\hat{a}_i - \alpha_i(\dot{x}_i - \hat{v}_i)) + \frac{d}{dt}[(I_{p_i} - J_i^\sharp J_i)\varphi_i]. \tag{3}$$

Let $\zeta_i = \mathrm{col}(\hat{x}_i, \hat{v}_i, \hat{a}_i) \in \mathbb{R}^{3m}$. Then for $i, j \in \mathcal{V}$, we define

$$\sigma_{ij} = \zeta_i - \zeta_j, \tag{4}$$

especially, $\sigma_i = \zeta_i - \mathrm{col}(x_0, v_0, a_0)$.

Let $\hat{s}_i = \dot{q}_i - \dot{\hat{q}}_{ri}$. In the presence of uncertain dynamics and input disturbance, the DCEA for MHMs consist of the control law

$$u_i = Y_i(q_i, \dot{q}_i, \dot{\hat{q}}_{ri}, \ddot{\hat{q}}_{ri})\hat{\vartheta}_i - J_i^T \mathcal{K}_{xi} J_i \hat{s}_i - \mathcal{K}_{si}\hat{s}_i - \mathcal{K}_{ri}\mathrm{sgn}(\hat{s}_i), \tag{5}$$

and the distributed adaptive estimators

$$\begin{cases} \dot{\hat{\vartheta}}_i = -\mathcal{T}_i Y_i^T(q_i, \dot{q}_i, \dot{\hat{q}}_{ri}, \ddot{\hat{q}}_{ri})\hat{s}_i, & \text{(6a)} \\ \dot{\zeta}_i = -\left(\begin{bmatrix} \beta_1 & & \\ & \beta_2 & \\ & & \beta_3 \end{bmatrix} \otimes I_m\right) \mathrm{sgn}\left(\sum_{j\in\mathcal{N}_i} \varepsilon_{ij}\sigma_{ij} + b_i\sigma_i\right), & \text{(6b)} \end{cases}$$

where β_1, β_2 and β_3 are given in Assumption A2, $\otimes$ denotes the Kronecker product, σ_{ij} is given in (4), $\hat{\vartheta}_i$ is the estimated value of ϑ_i, $Y_i(q_i, \dot{q}_i, \dot{\hat{q}}_{ri}, \ddot{\hat{q}}_{ri})\hat{\vartheta}_i = \hat{H}_i(q_i)\ddot{\hat{q}}_{ri} + \hat{C}_i(q_i, \dot{q}_i)\dot{\hat{q}}_{ri} + \hat{g}_i(q_i)$, $\hat{H}_i(q_i)$, $\hat{C}_i(q_i, \dot{q}_i)$, and $\hat{g}_i(q_i)$ are the estimates of $H_i(q_i)$, $C_i(q_i, \dot{q}_i)$, and $g_i(q_i)$ respectively, $\mathcal{K}_{si}$, $\mathcal{K}_{ri} \in \mathbb{R}^{p_i \times p_i}$ and $\mathcal{K}_{xi} \in \mathbb{R}^{m\times m}$ are positive definite matrices, $\mathcal{T}_i$ is a designed diagonal positive definite matrix with an appropriate dimension.

Remark 4. *It can be seen from the definition of $J_i^\sharp$ that $I_{p_i} - J_i^\sharp J_i = 0$ for $i \in \mathcal{E}$. Therefore, (2) implies that for redundant manipulators and nonredundant ones, $\dot{\hat{q}}_{ri}$ is distinguishing, namely,*

$$\dot{\hat{q}}_{ri} = \begin{cases} J_i^{-1}(\hat{v}_i - \alpha_i(x_i - \hat{x}_i)), & i \in \mathcal{E}, \\ J_i^\dagger(\hat{v}_i - \alpha_i(x_i - \hat{x}_i)) + (I_{p_i} - J_i^\dagger J_i)\varphi_i, & i \in \mathcal{F}. \end{cases}$$

Besides, $\ddot{\hat{q}}_{ri}$ is distinguishing with respect to redundant manipulators and nonredundant ones. It follows that the control law (5) is distinguishingly designed with respect to different sets of manipulators.

3.2. Boundedness Analysis

In this section, by analyzing the boundedness of the system states, the simplification of the close-loop dynamics is given.

The normal variables $\dot{q}_{ri}$, $\ddot{q}_{ri}$ and s_i with respect to the auxiliary variables $\dot{\hat{q}}_{ri}$, $\ddot{\hat{q}}_{ri}$ and $\hat{s}_i$, containing estimated states, are defined as

$$\begin{aligned} \dot{q}_{ri} &= J_i^\sharp(v_0 - \alpha_i(x_i - x_0)) + (I_{p_i} - J_i^\sharp J_i)\varphi_i, \\ \ddot{q}_{ri} &= \dot{J}_i^\sharp(v_0 - \alpha_i(x_i - x_0)) + J_i^\sharp(a_0 - \alpha_i(\dot{x}_i - v_0)) + \tfrac{d}{dt}[(I_{p_i} - J_i^\sharp J_i)\varphi_i], \\ s_i &= \dot{q}_i - \dot{q}_{ri}, \end{aligned} \tag{7}$$

where the normal variables are formed based on the estimated variables by replacing $\hat{x}_i$, $\hat{v}_i$ and $\hat{a}_i$ with x_0, v_0 and a_0 respectively. Then we define

$$\begin{aligned} \dot{\tilde{q}}_{ri} &= \dot{\hat{q}}_{ri} - \dot{q}_{ri} \\ &= J_i^\sharp(\hat{v}_i - v_0 + \alpha_i(\hat{x}_i - x_0)), \end{aligned} \tag{8}$$

and

$$\begin{aligned} \ddot{\tilde{q}}_{ri} &= \ddot{\hat{q}}_{ri} - \ddot{q}_{ri} \\ &= \dot{J}_i^\sharp(\hat{v}_i - v_0 + \alpha_i(\hat{x}_i - x_0)) + J_i^\sharp(\hat{a}_i - a_0 + \alpha_i(\hat{v}_i - v_0)). \end{aligned} \tag{9}$$

Let $\tilde{s}_i = \hat{s}_i - s_i = -\dot{\tilde{q}}_{ri}$. Substituting (5) into (1) yields the following

close-loop dynamics

$$\begin{aligned} &H_i(q_i)\dot{s}_i + C_i(q_i,\dot{q}_i)s_i + d_i(t) + J_i^T\mathcal{K}_{xi}J_i s_i + \mathcal{K}_{si}s_i + \mathcal{K}_{ri}\mathrm{sgn}(s_i) \\ &\quad = Y_i(q_i,\dot{q}_i,\dot{q}_{ri},\ddot{q}_{ri})\tilde{\vartheta}_i + \tilde{f}_i(t), \end{aligned} \tag{10}$$

where $\tilde{\vartheta}_i = \hat{\vartheta}_i - \vartheta_i$ and $\tilde{f}_i(t) = \hat{H}_i(q_i)\ddot{\tilde{q}}_{ri} + \hat{C}_i(q_i,\dot{q}_i)\dot{\tilde{q}}_{ri} - J_i^T\mathcal{K}_{xi}J_i\tilde{s}_i - \mathcal{K}_{si}\tilde{s}_i - \mathcal{K}_{ri}[\mathrm{sgn}(\hat{s}_i) - \mathrm{sgn}(s_i)]$. The boundedness of the states $q_i(t)$, $\dot{q}_i(t)$, $s_i(t)$, and $\tilde{f}_i(t)$, which will be used hereinafter, is analyzed in the following theorem.

Theorem 1. *Suppose that Assumptions A1 and A2 hold. The distributed sliding-mode estimator (6b) guarantees that there exists a settle time $t_f \in (t_0,\infty)$ such that $\tilde{f}_i(t) = 0$ when $t \geq t_f$, $\forall i \in \mathcal{V}$. Moreover, using the DCEA (5) and (6) for (1), the states $q_i(t)$, $\dot{q}_i(t)$, and $s_i(t)$ will remain bounded for bounded initial values when $t \in \mathcal{Q}_f = [t_0, t_f)$.*

Proof. For the first presentation, we prove that there exists a finite time $t_f \in (t_0,\infty)$ such that $\tilde{f}_i(t) = 0$ when $t \geq t_f$. Because the right-hand side of (6b) is discontinuous, the differential inclusions and nonsmooth analysis are invoked for convergence analysis of (6b) [40, 41]. The error dynamics of (6b) can be rewritten as

$$\dot{\sigma}_i \in^{a.e.} \mathbb{K}\left\{ -\left(\begin{bmatrix} \beta_1 & & \\ & \beta_2 & \\ & & \beta_3 \end{bmatrix} \otimes I_m \right) \mathrm{sgn}\left(\sum_{j\in\mathcal{N}_i} \varepsilon_{ij}\sigma_{ij} + b_i\sigma_i \right) - \begin{bmatrix} \dot{x}_0 \\ \dot{v}_0 \\ \dot{a}_0 \end{bmatrix} \right\},$$

where *a.e.* stands for "almost everywhere" refer to almost all $t \in \mathcal{Q}$, and $\mathbb{K}\{\cdot\}$ denotes the differential inclusion [41]. By Theorem 3.1 in [14], under Assumptions A1 and A2, it can be obtained that $\sigma_i = 0$ when $t \geq t_f$ and t_f is bounded by

$$t_f \leq t_{f\max} := \max(t_{f1}, t_{f2}, t_{f3}) < \infty,$$

$$t_{f1} = t_0 + \frac{\max_{i\in\mathcal{V}} \|\hat{x}_i(t_0) - x_0(t_0)\|_\infty}{\beta_1 - \sup_{t\in\mathcal{Q}} \|v_0\|_\infty},$$

$$t_{f2} = t_0 + \frac{\max_{i\in\mathcal{V}} \|\hat{v}_i(t_0) - v_0(t_0)\|_\infty}{\beta_2 - \sup_{t\in\mathcal{Q}} \|a_0\|_\infty},$$

$$t_{f3} = t_0 + \frac{\max_{i\in\mathcal{V}} \|\hat{a}_i(t_0) - a_0(t_0)\|_\infty}{\beta_3 - \sup_{t\in\mathcal{Q}} \|\dot{a}_0\|_\infty},$$

where $\max(\cdot)$ and $\sup(\cdot)$ denote the maximal value and the supremum respectively. It follows from (8) and (9) that $\dot{\tilde{q}}_{ri} = 0$ and $\ddot{\tilde{q}}_{ri} = 0$ when $t \geq t_f$.

Therefore, $\tilde{f}_i(t) = 0$ when $t \geq t_f$, $\forall i \in \mathcal{V}$.

For the second presentation, using the DCEA (5) and (6) for (1), it is shown that the states $q_i(t)$, $\dot{q}_i(t)$, and $s_i(t)$ will remain bounded for bounded initial values when $t \in \mathcal{Q}_f$. Note that

$$\left\| \begin{bmatrix} \beta_1 & & \\ & \beta_2 & \\ & & \beta_3 \end{bmatrix} \otimes I_m \right\|_\infty \leq \max(\beta_1, \beta_2, \beta_3),$$

and

$$\left\| \text{sgn}\left(\sum_{j \in \mathcal{N}_i} \varepsilon_{ij} \sigma_{ij} + b_i \sigma_i \right) \right\|_\infty \leq 1.$$

It thus follows from (6b) that

$$\left\| \dot{\zeta}_i \right\|_\infty \leq \max(\beta_1, \beta_2, \beta_3), \ \forall i \in \mathcal{V},$$

which means

$$\sup_{t \in \mathcal{Q}_f} \left\| \zeta_i(t) \right\|_\infty \leq \max(\beta_1, \beta_2, \beta_3)(t_f - t_0) < \infty, \ \forall i \in \mathcal{V}.$$

It follows that $\hat{x}_i(t)$, $\hat{v}_i(t)$, and $\hat{a}_i(t)$ remain bounded for bounded initial values $\hat{x}_i(t_0)$, $\hat{v}_i(t_0)$, and $\hat{a}_i(t_0)$ when $t \in \mathcal{Q}_f$. For bounded q_i and $\dot{q}_i$, the kinematics in (1) implies that x_i and $\dot{x}_i$ remain bounded. Then (2) and (3) implies that $\dot{\hat{q}}_{ri}$, $\ddot{\hat{q}}_{ri}$ and $\hat{s}_i$ remain bounded for bounded q_i and $\dot{q}_i$. By (7)-(9), $\dot{q}_{ri}$, $\ddot{q}_{ri}$, s_i, $\dot{\tilde{q}}_{ri}$, $\ddot{\tilde{q}}_{ri}$, and $\tilde{s}_i$ remain bounded for bounded q_i and $\dot{q}_i$. By Property P2 and Remark 1, $Y_i(q_i, \dot{q}_i, \dot{\hat{q}}_{ri}, \ddot{\hat{q}}_{ri})$ are bounded for bounded q_i and $\dot{q}_i$. Then (6a) implies $\hat{\vartheta}_i(t)$ remain bounded when $t \in \mathcal{Q}_f$ for bounded initial value $\hat{\vartheta}_i(t_0)$. It follows that $\tilde{f}_i(t)$ remain bounded for bounded q_i and $\dot{q}_i$. By (10), $\dot{s}_i$ remains bounded for bounded q_i and $\dot{q}_i$. Therefore, we can get that for bounded initial values $q_i(t_0)$ and $\dot{q}_i(t_0)$, the states $q_i(t)$, $\dot{q}_i(t)$, and $s_i(t)$ remain bounded when $t \in \mathcal{Q}_f$. This completes the proof. □

3.3. Convergence Analysis

In this section, based on Theorem 1, the convergence of the close-loop dynamics is analyzed. Differential inclusion and Filippov solution [41] are invoked because the presented DCEA are nonsmooth.

By Theorem 1, $\hat{s}_i = s_i$ and $\tilde{f}_i(t) = 0$ when $t \in \bar{\mathcal{Q}}_f = [t_f, \infty)$. Then when $t \in \bar{\mathcal{Q}}_f$, the combination of (6) and (10) yields the following cascade system

$$\begin{cases} \dot{s}_i = H_i^{-1}(q_i)[-C_i(q_i, \dot{q}_i)s_i - J_i^T \mathcal{K}_{xi} J_i s_i - \mathcal{K}_{si} s_i \\ \qquad\qquad + Y_i(q_i, \dot{q}_i, \dot{q}_{ri}, \ddot{q}_{ri})\tilde{\vartheta}_i + \tilde{h}_i(t)], \\ x_i = \psi_i(q_i), \ \dot{x}_i = J_i \dot{q}_i, \\ \dot{\hat{\vartheta}}_i = -\mathcal{T}_i Y_i^T(q_i, \dot{q}_i, \dot{q}_{ri}, \ddot{q}_{ri}) s_i, \end{cases} \tag{11}$$

where $q_i(t_f)$, $\dot{q}_i(t_f)$, $x_i(t_f)$, $\dot{x}_i(t_f)$, and $s_i(t_f)$ are bounded, $\tilde{h}_i(t) = -d_i(t) - \mathcal{K}_{ri}\mathrm{sgn}(s_i)$ denotes the combination of the nonsmooth and uncertain terms in the system dynamics. Then the following theorem is given.

Theorem 2. *Suppose that Assumptions A1 and A2 hold. Using the DCEA (5) and (6) for (1), if* $\lambda_{\min}(\mathcal{K}_{xi}) > 0$, $\lambda_{\min}(\mathcal{K}_{si}) > 0$, $\lambda_{\min}(\mathcal{K}_{ri}) \geq \sup_{t\in\mathcal{Q}} \|d_i(t)\|$, *and* $\lambda_{\min}(\mathcal{T}_i) > 0$, *then the control tasks in this paper can be achieved, namely,* $x_i \to x_0$ *and* $\dot{x}_i \to v_0$ *as* $t \to \infty$, $\forall i \in \mathcal{V}$; $e_{si} \to 0$ *as* $t \to \infty$, $\forall i \in \mathcal{F}$.

Proof. The proof proceeds in three steps. First, the passivity of the close-loop dynamics (11) is analyzed. Second, the convergence of s_i and $J_i s_i$ is obtained using differential inclusions and nonsmooth analysis. Finally, the stability of x_i and e_{si} is shown invoking kinematic analysis of nonredundant and redundant manipulators.

The first presentation presents the passivity of the close-loop dynamics. For system (11), consider the following storage function

$$V_{i1} = \frac{1}{2}(s_i^T H_i(q_i) s_i + \tilde{\vartheta}_i^T \mathcal{T}_i^{-1} \tilde{\vartheta}_i).$$

Differentiating the storage function along (11) gives

$$\begin{aligned} \dot{V}_{i1} &= \tfrac{1}{2} s_i^T \dot{H}_i(q_i) s_i + s_i^T H_i(q_i) \dot{s}_i + \tilde{\vartheta}_i^T \mathcal{T}_i^{-1} \dot{\hat{\vartheta}}_i \\ &= -s_i^T \mathcal{K}_{si} s_i - s_i^T J_i^T(q_i) \mathcal{K}_{xi} J_i(q_i) s_i + s_i^T \tilde{h}_i \\ &\leq s_i^T \tilde{h}_i, \end{aligned}$$

where Property P1 is invoked to obtain the second equation. Integrating

both sides of the above inequality with respect to time $t \in \bar{\mathcal{Q}}_f$ provides

$$V_{i1}(t) - V_{i1}(t_f) \leq \int_{t_f}^{t} s_i^T(\omega)\tilde{h}_i(\omega)d\omega. \tag{12}$$

It thus follows that system (11) is passive with the mapping from the input $\tilde{h}_i(t)$ to the state s_i, $\forall i \in \mathcal{V},\ t \in \bar{\mathcal{Q}}_f$ [42].

The second presentation analyze the convergence of s_i and $J_i s_i$ using nonsmooth analysis and the passivity property given in the first presentation. Let $\eta_i \in (0, \lambda_{\min}(\mathcal{K}_{xi}))$ be a positive scalar. Then when $t \in \bar{\mathcal{Q}}_f$, consider the Lyapunov function candidate for system (11) as

$$V_i = V_{i1} + \eta_i \int_{t_f}^{t} s_i^T(\omega) J_i^T(q_i(\omega)) J_i(q_i(\omega)) s_i(\omega) d\omega.$$

Considering that $\tilde{h}_i(t)$ is nonsmooth and uncertain, the generalized time derivative is invoked to carry out more formal mathematical analysis; additionally, considering that the signum function is measurable and locally essentially bounded, the Filippov solution exists for (11) [40, 41]. Taking the generalized time derivative of V_i along (11) gives that

$$\begin{aligned}
\dot{\tilde{V}}_i &= \mathbb{K}\{\tfrac{1}{2} s_i^T \dot{H}_i(q_i) s_i + s_i^T [-C_i(q_i, \dot{q}_i) s_i - J_i^T \mathcal{K}_{xi} J_i s_i - \mathcal{K}_{si} s_i \\
&\quad + Y_i(q_i, \dot{q}_i, \dot{q}_{ri}, \ddot{q}_{ri})\tilde{\vartheta}_i + \tilde{h}_i(t)] - \tilde{\vartheta}_i^T Y_i^T(q_i, \dot{q}_i, \dot{q}_{ri}, \ddot{q}_{ri}) s_i \\
&\quad + \eta_i s_i^T J_i^T J_i s_i\} \\
&= \mathbb{K}\{-s_i^T \mathcal{K}_{si} s_i - s_i^T J_i^T (\mathcal{K}_{xi} - \eta_i I_m) J_i s_i - s_i^T \mathcal{K}_{ri} \mathrm{sgn}(s_i) - s_i^T d_i\} \\
&\leq -s_i^T \mathcal{K}_{si} s_i - s_i^T J_i^T (\mathcal{K}_{xi} - \eta_i I_m) J_i s_i - \|s_i\|(\lambda_{\min}(\mathcal{K}_{ri}) - \|d_i\|) \\
&\leq -s_i^T \mathcal{K}_{si} s_i - s_i^T J_i^T (\mathcal{K}_{xi} - \eta_i I_m) J_i s_i - \|s_i\|(\lambda_{\min}(\mathcal{K}_{ri}) - \sup_{t \in \mathcal{Q}} \|d_i(t)\|) \\
&\leq -s_i^T \mathcal{K}_{si} s_i - s_i^T J_i^T (\mathcal{K}_{xi} - \eta_i I_m) J_i s_i,
\end{aligned}$$

where (12), $\lambda_{\min}(\mathcal{K}_{ri}) \geq \sup_{t \in \mathcal{Q}} \|d_i(t)\|$, Property P1-P3, and the fact that $\mathbb{K}\{f\} \equiv \{f\}$ if f is continuous [41] are invoked to obtain the above inequalities. Provided $\lambda_{\min}(\mathcal{K}_{xi}) > 0$ and $\lambda_{\min}(\mathcal{K}_{si}) > 0$, $\dot{\tilde{V}}_i$ is negative definite, $\forall i \in \mathcal{V}$. It follows that $V_i \in \mathcal{L}_\infty$; then $s_i, J_i s_i, \tilde{\vartheta}_i \in \mathcal{L}_\infty$, $\forall i \in \mathcal{V}$. $\tilde{\vartheta}_i \in \mathcal{L}_\infty$ implies that $\hat{\vartheta}_i \in \mathcal{L}_\infty$ because ϑ_i is a vector of constant dynamic parameters,

$\forall i \in \mathcal{V}$. $s_i, J_i s_i \in \mathcal{L}_\infty$ gives that $Y_i(q_i, \dot{q}_i, \dot{q}_{ri}, \ddot{q}_{ri}) \in \mathcal{L}_\infty$, $\forall i \in \mathcal{V}$. Then (5) and (6) imply that the control input u_i is bounded. Thus, the closed-loop dynamics (11) implies that $\dot{s}_i \in \mathcal{L}_\infty$; then s_i is uniformly continuous, $\forall i \in \mathcal{V}$. Then invoking Corollary 2 in [41], $s_i \to 0$ and $J_i s_i \to 0$ as $t \to \infty$, $\forall i \in \mathcal{V}$.

The third presentation shows that $e_{si} \to 0$ ($\forall i \in \mathcal{F}$) as $t \to \infty$ under the DCEA. Let $e_i = x_i - x_0$. (7) gives that

$$\dot{e}_i = -\alpha_i e_i + J_i s_i. \tag{13}$$

It thus follows from [42] that (13) is input-to-state stable with respect to the input $J_i(q_i)s_i$ and the state e_i; hence, $J_i s_i \to 0$ as $t \to \infty$ implies that $e_i \to 0$ as $t \to \infty$, which means $x_i \to x_0$ and $\dot{x}_i \to v_0$ as $t \to \infty$, $\forall i \in \mathcal{V}$, *i.e.*, the maintask is addressed. Additionally, by (7) and Lemma 1, for the redundant manipulators, namely, for $i \in \mathcal{F}$,

$$\begin{aligned} e_{si} &= (I_{p_i} - J_i^\sharp J_i)(\dot{q}_i - \varphi_i) \\ &= (I_{p_i} - J_i^\sharp J_i)[\dot{q}_i - J_i^\sharp(v_0 - \alpha_i(x_i - x_0)) - (I_{p_i} - J_i^\sharp J_i)\varphi_i] \\ &= (I_{p_i} - J_i^\sharp J_i)(\dot{q}_i - \dot{q}_{ri}) \\ &= (I_{p_i} - J_i^\sharp J_i)s_i. \end{aligned}$$

Therefore, $s_i \to 0$ as $t \to \infty$ implies that $e_{si} \to 0$ as $t \to \infty$, $\forall i \in \mathcal{F}$, *i.e.*, the subtask is addressed. This completes the proof. □

Note that the necessary and sufficient condition can be obtained by some simple transformation for Theorem 2. The proof of Corollary 1 can be easily obtained by contradiction and is omitted here.

Corollary 1. *Suppose that* $\lambda_{\min}(\mathcal{K}_{xi}) > 0$, $\lambda_{\min}(\mathcal{K}_{si}) > 0$, $\lambda_{\min}(\mathcal{K}_{ri}) \geq \sup_{t\in\mathcal{Q}} \|d_i(t)\|$, $\lambda_{\min}(\mathcal{T}_i) > 0$, *and Assumption A2 holds. Using (5) and (6) for (1), the control tasks are achieved, namely,* $x_i \to x_0$ *and* $\dot{x}_i \to v_0$ *as* $t \to \infty$, $\forall i \in \mathcal{V}$; $e_{si} \to 0$ *as* $t \to \infty$, $\forall i \in \mathcal{F}$, *if and only if Assumption A1 holds.*

It is worthy to point out that the DCEA (5) and (6) can also deal with the consensus problem, namely, leaderless coordination, presented in [20] by some simple changes.

Corollary 2. *Suppose that $\mathcal{G}$ contains a spanning tree and Assumption A2 holds. Let estimators (6b) be replaced by*

$$\dot{\zeta}_i = -\left(\begin{bmatrix} \beta_1 & & \\ & \beta_2 & \\ & & \beta_3 \end{bmatrix} \otimes I_m\right) \operatorname{sgn}\left(\sum_{j\in\mathcal{N}_i} \varepsilon_{ij}\sigma_{ij}\right).$$

Using (5), (6a) and the above estimators for the MHMs (1), if $\lambda_{\min}(\mathcal{K}_{xi}) > 0$, $\lambda_{\min}(\mathcal{K}_{si}) > 0$, $\lambda_{\min}(\mathcal{K}_{ri}) \geq \sup_{t\in\mathcal{Q}} \|d_i(t)\|$, and $\lambda_{\min}(\mathcal{T}_i) > 0$, then consensus in [20] is achieved, meanwhile, the subtasks are obtained for $i \in \mathcal{F}$.

Let a switching topology $\mathcal{G}(t) = \{\mathcal{V}, \xi(t), \mathcal{A}(t)\}$ be the system interaction. $\mathcal{A}(t) = [\varepsilon_{ij}(t)]_{n\times n}$ is the weighted adjacency matrix. $\mathcal{B}(t) = [b_1(t), \ldots, b_n(t)]^T$ is the time-varying nonnegative weight vector between the n nodes and the leader. We can obtain the following corollary.

Corollary 3. *Suppose that Assumption A2 holds and the leader is reachable to the MHMs under $\mathcal{G}(t)$ and $\mathcal{B}(t)$. Let (6b) be replaced by*

$$\dot{\zeta}_i = -\left(\begin{bmatrix} \beta_1 & & \\ & \beta_2 & \\ & & \beta_3 \end{bmatrix} \otimes I_m\right) \operatorname{sgn}\left(\sum_{j\in\mathcal{N}_i} \varepsilon_{ij}(t)\sigma_{ij} + b_i(t)\sigma_i\right).$$

Using (5), (6a) and the above estimators for the MHMs (1), if $\lambda_{\min}(\mathcal{K}_{xi}) > 0$, $\lambda_{\min}(\mathcal{K}_{si}) > 0$, $\lambda_{\min}(\mathcal{K}_{ri}) \geq \sup_{t\in\mathcal{Q}} \|d_i(t)\|$, and $\lambda_{\min}(\mathcal{T}_i) > 0$, then $x_i \to x_0$ and $\dot{x}_i \to v_0$ as $t \to \infty$, $\forall i \in \mathcal{V}$; $e_{si} \to 0$ as $t \to \infty$, $\forall i \in \mathcal{F}$.

Proof. The proof can be easily developed by the combination of Lemma 6 in [43] and Theorem 2, and is omitted here. □

Assuming that $\mathcal{G}$ is balanced connected or detail balanced, other conditions are identical, the above results still hold, meanwhile, the subtasks are obtained for all $i \in \mathcal{F}$.

Remark 5. *The DCEA (5) and (6) provide a distributed control framework for various multi-agent networks. Note that (5) and* (6a) *deal with the tracking of the estimated value of the ith manipulator using its states (local states), and are called local algorithms, while (6b) deals with the estimation of the states of the leader using both the states of the ith manipulator and its neighbour set, and is called networked algorithms. Thus, the DCEA consists of local algorithms and networked algorithms, which can be easily applied*

to various nonlinear multi-agent networks by designing local algorithms and networked algorithms separately.

Remark 6. *Note that Assumption A1 is less conservative than many other assumptions in recent works. For details, let $\bar{\mathcal{G}}$ be the augmentation digraph by adding the leader and the weight vector $\mathcal{B}$ to $\mathcal{G}$, Assumption A1 means that $\bar{\mathcal{G}}$ contains a spanning tree, which is less conservative than the following assumptions for graphs, including strong connected [7, 31, 32], balanced connected [35], detail balanced [44], which means, less consumption is required to establish and maintain Assumption A1.*

Remark 7. *Assumption A1 implies that the presented DCEA have the following advantages. (1) If $\mathcal{G}$ contains one or more edges, then only partial nodes are required to be pinned, which reflects the superiority of networked control. (2) By weighing the cost of maintaining interaction and pinning nodes, the interaction topology can be optimized.*

Remark 8. *It is worthy to point out that the leader considered in Theorem 2 is a bounded time-varying signal, which is necessary and inevitable in some natural and man-made systems, e.g., humanoid hands and multi-fingered hands [11, 12].*

4. Simulations

In this section, simulations are performed to show the effectiveness of the presented DCEA. The MHMs contain five two-DOF and two three-DOF planar manipulators, as shown in Fig.1, and the physical parameters are given in Tab.1. The dynamics and kinematics of the MHMs are adopted from [31]. The input disturbance $d_i(t)$ is a stochastic signal, whose ∞-norm is bounded by 40. The maintask is to obtain the tracking of the leader

$$x_0(t) = \begin{bmatrix} 1.2 + 0.5\sin(\pi t) \\ 1.3 + 0.3\cos(\pi t) \end{bmatrix} \tag{14}$$

for the end-effectors in the XY plane. The MHMs are interacted invoking the digraph $\mathcal{G}$ shown in Fig.2, where node 0 is the leader, nodes 1-5 are two-DOF nonredundant manipulators, nodes 6 and 7 are three-DOF redundant manipulators, and nodes 1, 3, 5, and 7 can access the information of the leader directly. For simplification, if node i can access the information of node j

directly, $\varepsilon_{ij} = 1$; otherwise $\varepsilon_{ij} = 0$, $\forall i, j = 1, \ldots, 7$. $\mathcal{B} = \text{col}(1, 0, 1, 0, 1, 0, 1)$. The Laplacian matrix with respect to the digraph $\mathcal{G}$ is given by

$$\mathcal{L} = \begin{bmatrix} 0 & 0 & 0 & 0 & 0 & 0 & 0 \\ -1 & 2 & -1 & 0 & 0 & 0 & 0 \\ 0 & 0 & 0 & 0 & 0 & 0 & 0 \\ -1 & 0 & -1 & 2 & 0 & 0 & 0 \\ 0 & 0 & 0 & 0 & 0 & 0 & 0 \\ 0 & 0 & 0 & 0 & -1 & 1 & 0 \\ 0 & 0 & 0 & 0 & 0 & 0 & 0 \end{bmatrix}.$$

The elements of $q_i(0)$, $\dot{q}_i(0)$, and $\zeta_i(0)$ are randomly chosen from $[-5, 5]$. The elements of $\hat{\vartheta}_i(0)$ are randomly selected from $[0, 5]$. The control parameters for the DCEA (5) and (6) are given by

$$\begin{array}{l} \beta_1 = 4,\ \beta_2 = 7,\ \beta_3 = 21; \\ \alpha_i = 3,\ \mathcal{T}_i = 0.1I,\ \mathcal{K}_{xi} = diag\{50, 50\},\ \forall i = 1, \ldots, 7; \\ \mathcal{K}_{si} = diag\{100, 100\},\ \mathcal{K}_{ri} = diag\{60, 60\},\ \forall i = 1, \ldots, 5; \\ \mathcal{K}_{si} = diag\{150, 150, 150\},\ \mathcal{K}_{ri} = diag\{60, 60, 60\},\ \forall i = 6, 7, \end{array}$$

where I denotes the identity matrices of appropriate orders. The sampling period is selected as 10 ms.

i-th node	m_i (kg)	l_i (m)	r_i (m)	I_i $(kg \cdot m^2)$
$i = 1$	0.8, 0.6	1.4, 0.9	0.8, 0.45	6, 3
$i = 2$	1, 0.8	1.2, 1.1	0.7, 0.5	2, 3
$i = 3$	0.5, 0.8	1.1, 1.3	0.4, 0.6	5, 3
$i = 4$	1.5, 0.8	1.1, 1.2	0.6, 0.6	5, 4
$i = 5$	2.3, 0.8	1.0, 1.2	0.4, 0.7	5, 3
$i = 6$	0.8, 1.2, 1.4	0.8, 1.1, 1.4	0.4, 0.5, 0.7	4, 6, 5
$i = 7$	1.8, 1.2, 1.4	1, 1.1, 1.2	0.6, 0.6, 0.6	5, 6, 5

Table 1: The physical parameters of the MHMs.

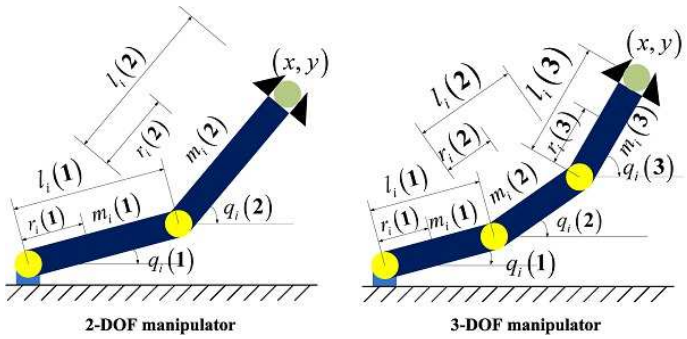

Figure 1: The mechanical structure of the individuals in the MHMs.

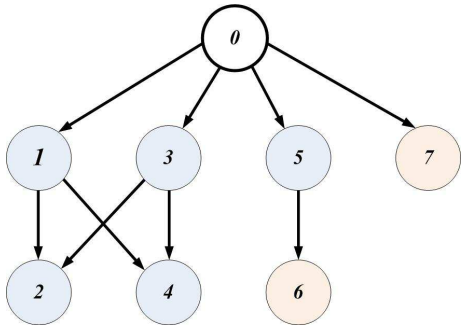

Figure 2: The interaction of MHMs $\mathcal{G}$.

Simulation results of the presented DCEA are shown in Fig.3-7. (14) implies that $\|v_0\|_\infty \leq 1.571$, $\|a_0\|_\infty \leq 4.935$, and $\|\dot{a}_0\|_\infty \leq 15.504$. It thus follows from Fig.2 that Assumptions A1 and A2 holds in this simulation. Then the estimated states $\hat{x}_i$, $\hat{v}_i$ and $\hat{a}_i$ follows the states of the leader in finite time, as shown in Fig.3. It gives that $\tilde{f}_i(t)$ converges to the origin in finite time and Theorem 1 holds, which means the distributed sliding-mode estimator (6b) can drive the system dynamics into the cascade form (11). Moreover, the end-effectors of the manipulators follows the leader asymptotically because $\lambda_{\min}(\mathcal{K}_{xi}) > 0$, $\lambda_{\min}(\mathcal{K}_{si}) > 0$ and $\lambda_{\min}(\mathcal{K}_{ri}) \geq \sup_{t\in\mathcal{Q}} \|d_i(t)\|$, as shown in Fig.4 (the trajectories of the states in time-domain) and Fig.5 (the trajectories of the states in XY plane). It means that the maintask can be accomplished under the DCEA in the simulations. The subtask function for the sixth manipulator (node 6) is selected as $\varphi_6 = \text{col}[0, 9(1-q_2), 0]$ with respect to the performance indices $4.5(q_2-1)^2$, where q_2 denotes the second joint angle of the sixth manipulator. This subtask function forces the

second joint of the sixth manipulator toward 1 rad. For Fig.6, in the left picture, the second joint of the sixth manipulator is forced toward 1 rad with subtask control; in the right picture, the subtask cannot be accomplished without subtask control. The subtask function for the seventh manipulator is $\varphi_7 = \frac{\partial}{\partial q}\left(\det(J_7 J_7^T)\right)$, where q denotes the joint position of the seventh manipulator. This subtask function increases the manipulability of the seventh manipulator, as shown in [39]. It can be observed in Fig.7 that the manipulability of the seventh manipulator is enhanced with subtask control. It means that the subtask can also be accomplished under the DCEA in the simulations.

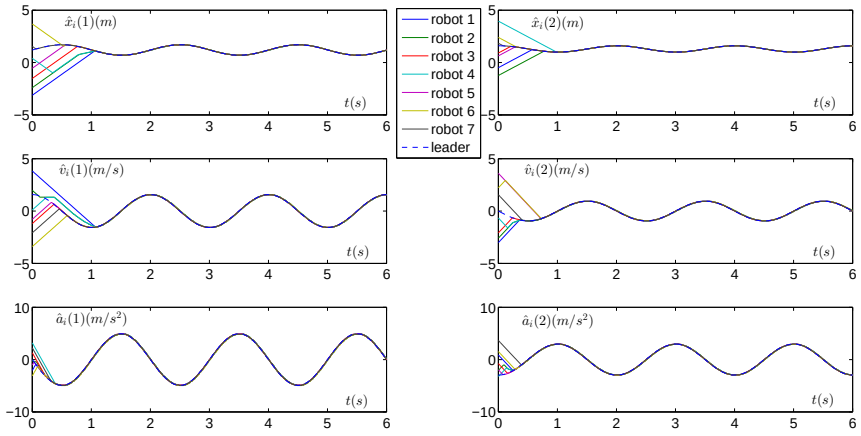

Figure 3: The estimated value $\hat{x}_i$, $\hat{v}_i$ and $\hat{a}_i$ for the ith manipulator.

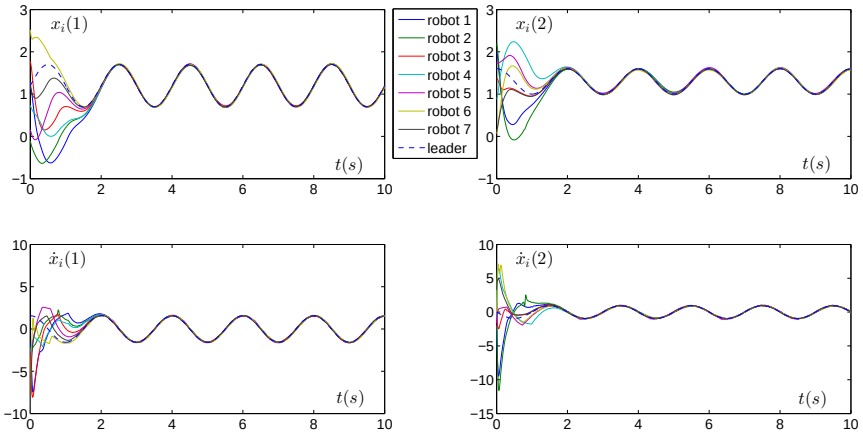

Figure 4: The task-space states x_i and $\dot{x}_i$ for the ith manipulator.

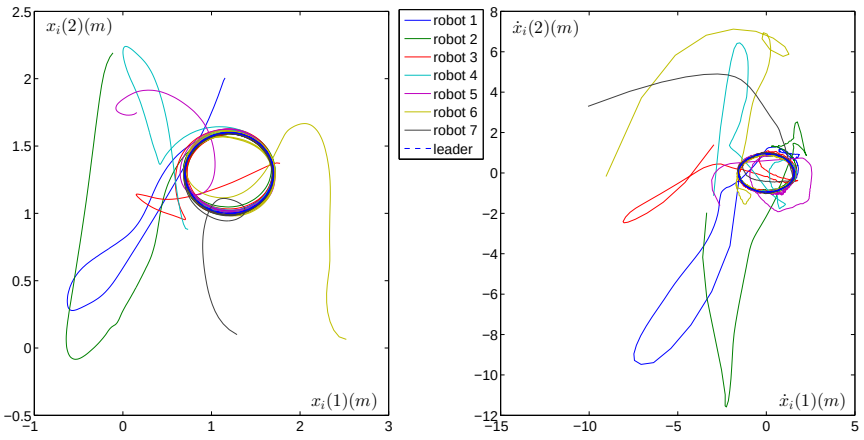

Figure 5: Position (the left picture) and velocity (the right picture) of the end-effectors of MHMs in the XY plane.

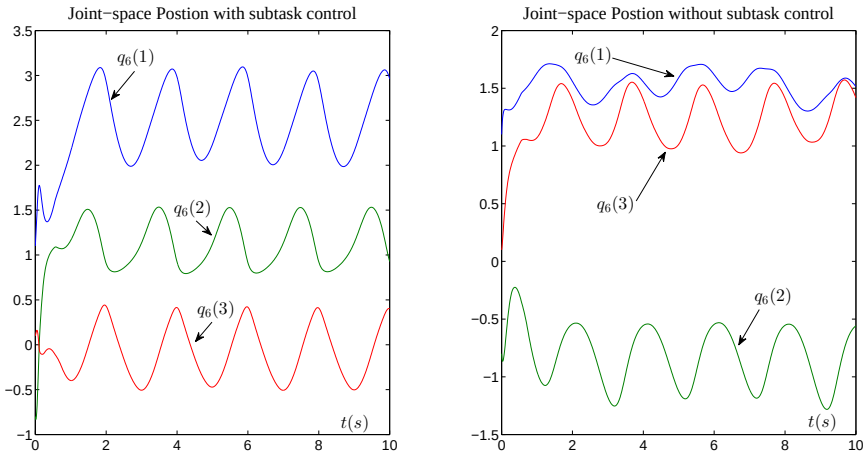

Figure 6: Joint-space position of the sixth manipulator with and without subtask control.

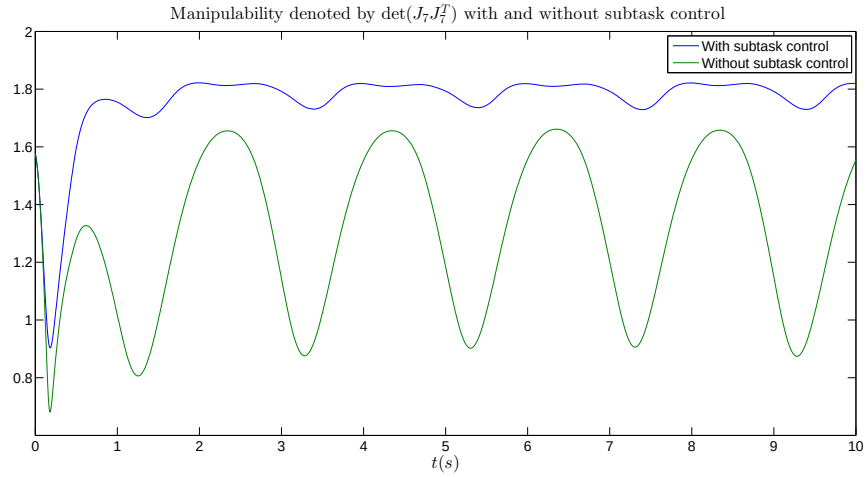
Manipulability denoted by $\det(J_7 J_7^T)$ with and without subtask control
With subtask control
Without subtask control
$t(s)$

Figure 7: Manipulability of the seventh manipulator with and without subtask control.

5. Conclusion

This paper focus on the task-space coordinated tracking problem of MHMs with parametric uncertainties and input disturbances under digraphs. Especially, maintask and subtask for MHMs are designed and addressed simultaneously. Several conditions (including necessary and sufficient conditions,

sufficient conditions) for driving both the task-space tracking error and the subtask tracking error of MHMs to zero have been derived. The simulations for the DCEA have shown satisfactory performance in the MHMs containing two-DOF and three-DOF manipulators.

Acknowledgements

This work was supported in part by the National Natural Science Foundation of China under Grant 61272069.

References

[1] Y.C. Liu, Task-space coordination control of bilateral human-swarm systems, J. Frankl. Inst. 352 (1) (2015) 311-331.

[2] Z. Li, C.Y. Su, Neural-adaptive control of single-master-multiple-slaves teleoperation for coordinated multiple mobile manipulators with time-varying communication delays and input uncertainties, IEEE Trans. Neural Netw. Learn. Syst. 24 (9) (2013) 1400-1413.

[3] Y. Yang, C. Hua, X. Guan, Adaptive fuzzy finite-time coordination control for networked nonlinear bilateral teleoperation system, IEEE Trans. Fuzzy Syst. 22 (3) (2014) 631-641.

[4] Z. Lu, P. Huang, Z. Liu, Z. Meng, Stability conditions for asymmetric dual-user shared control method with uncertain time delay, IEEE International Conference on Information and Automation, 2015, pp. 1997-2002.

[5] Z. Lu, P. Huang, Kinesthetic performance analysis of asymmetric dual-user shared teleoperation system, 12th International Conference on Ubiquitous Robots and Ambient Intelligence (URAI), 2015, pp. 273-278.

[6] P. Huang, Z. Lu, Auxiliary asymmetric dual-user shared control method for teleoperation, 12th International Conference on Ubiquitous Robots and Ambient Intelligence (URAI), 2015, pp. 267-272.

[7] Y.C. Liu, Robust synchronisation of networked Lagrangian systems and its applications to multi-robot teleoperation, IET Control Theory Appl. 9 (1) (2015) 129-139.

[8] C. Hua, Y. Yang, P. X. Liu, Output-feedback adaptive control of networked teleoperation system with time-varying delay and bounded inputs, IEEE/ASME Trans. Mechatronics 20 (5) (2015) 2009-2020.

[9] Z. Li, L. Ding, H. Gao, G. Duan, C.Y. Su, Trilateral teleoperation of adaptive fuzzy force/motion control for nonlinear teleoperators with communication random delays. IEEE Trans. Fuzzy Syst. 21 (4) (2013) 610-624.

[10] Z. Li, Y. Xia, F. Sun, Adaptive fuzzy control for multilateral cooperative teleoperation for multiple robotic manipulators under random network-induced delays. IEEE Trans. Fuzzy Syst. 22 (2) (2014) 437-450.

[11] M.F. Ge, Z.H. Guan, T.Li, D.X. Zhang, R.Q. Liao, Robust mode-free sliding mode control of multi-fingered hand with position synchronization in the task space, Intelligent Robotics and Applications, Springer Berlin Heidelberg, 2012, pp. 571-580.

[12] W. Gueaieb, S. Al-Sharhan, M. Bolic, Robust computationally efficient control of cooperative closed-chain manipulators with uncertain dynamics, Automatica 43 (5) (2007) 842-851.

[13] R. Olfati-Saber, R.M. Murray, Consensus problems in networks of agents with switching topology and time-delays, IEEE Trans. Autom. Control 49 (9) (2004) 1520-1533.

[14] Y.C. Cao, W. Ren, Z.Y. Meng, Decentralized finite-time sliding mode estimators and their applications in decentralized finite-time formation tracking, Syst. Contr. Lett. 59 (9) (2010) 522-529.

[15] J. Li, D.W.C. Ho, J. Li, Distributed adaptive repetitive consensus control framework for uncertain nonlinear leader-follower multi-agent systems, J. Frankl. Inst. 352 (11) (2015) 5342-5360.

[16] H. Zhang, R. Yang, H. Yan, Q. Chen, Distributed event-triggered control for consensus of multi-agent systems, J. Frankl. Inst. 352 (9) (2015) 3467-3488.

[17] M.F. Ge, Z.H. Guan, B. Hu, D.X. He, R.Q. Liao, Distributed controller-estimator for target tracking of networked robotic systems under sampled interaction, Automatica 69 (2016) 410-417.

[18] M.F. Ge, Z.H. Guan, C. Yang, T. Li, Y.W. Wang. Time-varying formation tracking of multiple manipulators via distributed finite-time control. Neurocomputing 202 (2016) 20-26.

[19] Z. Li, Z. Chen, J. Fu, C. Sun, Direct adaptive controller for uncertain MIMO dynamic systems with time-varying delay and dead-zone inputs, Automatica 63 (2016) 287-291.

[20] Z.H. Guan, Z.W. Liu, G. Feng, M. Jian, Impulsive consensus algorithms for second-order multi-agent networks with sampled information, Automatica 48 (7) (2012) 1397-1404.

[21] Z.W. Liu, Z.H. Guan, X.M. Shen, G. Feng, Consensus of multi-agent networks with aperiodic sampled communication via impulsive algorithms using position-only measurements, IEEE Trans. Autom. Control 57 (10) (2012) 2639-2643.

[22] Z.H. Guan, B. Hu, M. Chi, D.X. He, X.M. Cheng, Guaranteed performance consensus in second-order multi-agent systems with hybrid impulsive control, Automatica 50 (9) (2014) 2415-2418.

[23] Z.W. Liu, X. Yu, Z.H. Guan, B. Hu, C. Li. Pulse-modulated intermittent control in consensus of multi-agent systems, IEEE Trans. Syst., Man, Cybern., Syst. (2016) DOI:10.1109/TSMC.2016.2524063.

[24] L. Ding, P. Yu, Z.W. Liu, Z.H. Guan, G. Feng. Consensus of second-order multi-agent systems via impulsive control using sampled hetero-information, Automatica 49 (9) (2013) 2881-2886.

[25] T. Imaida, K. Senda, Performance improvement of the PD-based bilateral teleoperators with time delay by introducing relative D-control, Advanced Robotics 29 (6) (2015) 385-400.

[26] N. Chopra, M.W. Spong, R. Lozano, Synchronization of bilateral teleoperators with time delay, Automatica 44 (8) (2008) 2142-2148.

[27] Y. Yang, C. Ge, H. Wang, X. Li, C. Hua, Adaptive neural network based prescribed performance control for teleoperation system under input saturation, J. Frankl. Inst. 352 (5) (2015) 1850-1866.

[28] S. Islam, P.X. Liu, A. El Saddik, Y.B. Yang, Bilateral control of teleoperation systems with time delay, IEEE-ASME Trans. Mechatronics 20 (1) (2015) 1-12.

[29] S.J. Chung, J.J.E. Slotine, Cooperative robot control and concurrent synchronization of Lagrangian systems, IEEE Trans. Robot. 25 (3) (2009) 686-700.

[30] J. Mei, W. Ren, B. Li, G. Ma, Distributed containment control for multiple unknown second-order nonlinear systems with application to networked Lagrangian systems, IEEE Trans. Neural Netw. Learn. Syst. 26 (9) (2015) 1885-1899.

[31] H.L. Wang, Passivity based synchronization for networked robotic systems with uncertain kinematics and dynamics, Automatica 49 (3) (2013) 755-761.

[32] H.L. Wang, Task-space synchronization of networked robotic systems with uncertain kinematics and dynamics, IEEE Trans. Autom. Control 58 (12) (2013) 3169-3174.

[33] E. Zergeroglu, D.D. Dawson, I.W. Walker, P. Setlur, Nonlinear tracking control of kinematically redundant robot manipulators, IEEE-ASME Trans. Mechatronics 9 (1) (2004) 129-132.

[34] W. Xu, J. Zhang, B. Liang, B. Li. Singularity analysis and avoidance for robot manipulators with non-spherical wrists, IEEE Trans. Ind. Electron. 63 (1) (2016) 277-290.

[35] Y.C. Liu, N. Chopra, Controlled synchronization of heterogeneous robotic manipulators in the task space, IEEE Trans. Robot. 28 (1) (2012) 268-275.

[36] Y. Nakamura, Advanced Robotics Redundancy and Optimization, Reading, MA: Addison-Wesley, 1991.

[37] R. Kelly, V. Santibanez, A. Loria, Control of robot manipulators in joint space, London: Springer, 2005.

[38] Z. Meng, D.V. Dimarogonas, K.H. Johansson, Leader-follower coordinated tracking of multiple heterogeneous Lagrange systems using continuous control, IEEE Trans. Robot. 30 (3) (2014) 739-745.

[39] P. Hsu, J. Hauser, S. Sastry, Dynamic control of redundant manipulators, J. Robot. Syst. 6 (1989) 133-148.

[40] B. Paden, S. Sastry, A calculus for computing Filippov's differential inclusion with application to the variable structure control of robot manipulators, IEEE Trans. Circuits Syst. CAS-34 (1) (1987) 73-82.

[41] N. Fischer, R. Kamalapurkar, W.E. Dixon, LaSalle-Yoshizawa corollaries for nonsmooth systems, IEEE Trans. Autom. Control, 58 (9) (2013) 2333-2338.

[42] H.K. Khalil, J.W. Grizzle, Nonlinear systems, New Jersey: Prentice hall, 1996.

[43] X. Wang, Y. Hong, Distributed finite-time χ-consensus algorithms for multi-agent systems with variable coupling topology, J. Syst. Sci. Complex 23 (2010) 209-218.

[44] X. Liu, J. Lam, W. Yu, G. Chen, Finite-time consensus of multiagent systems with a switching protocol, IEEE Trans. Neural Netw. Learn. Syst. 27 (4) (2016) 853-862.